2-Aminoethoxydiphenyl borate directly facilitates and indirectly inhibits STIM1-dependent gating of CRAC channels

Christine Peinelt, Annette Lis, Andreas Beck, Andrea Fleig and Reinhold Penner

Center for Biomedical Research at The Queen's Medical Center and John A. Burns School of Medicine at the University of Hawaii, Honolulu, HI 96813, USA

2-Aminoethoxydiphenyl borate (2-APB) has emerged as a useful pharmacological tool in the study of store-operated Ca^{2+} entry (SOCE). It has been shown to potentiate store-operated Ca^{2+} release-activated Ca^{2+} (CRAC) currents at low micromolar concentrations and to inhibit them at higher concentrations. Initial experiments with the three CRAC channel subtypes CRACM1, CRACM2 and CRACM3 have indicated that they might be differentially affected by 2-APB. We now present a thorough pharmacological profile of 2-APB and report that it can activate CRACM3 channels in a store-independent manner without the requirement of STIM1, whereas CRACM2 by itself is completely unresponsive to 2-APB and CRACM1 is only very weakly activated. However, when coexpressed with STIM1 and activated via store depletion, CRACM1 and CRACM2 are facilitated at low 2-APB concentrations and inhibited at higher concentrations, while CRACM3 only exhibits potentiated currents. Consistently, the 2-APB-induced CRAC currents exhibit altered selectivities that are characterized by a leftward shift in reversal potential and the emergence of large outward currents that are carried by normally impermeant monovalent cations such as Cs^+ or K^+. These results suggest that 2-APB has agonistic and antagonistic modes of action on CRAC channels, acting at the channel level as a store-independent and direct gating agonist for CRACM3 and a potentiating agonist for CRACM1 and CRACM2 following store-operated and STIM1-dependent activation. The inhibition of CRACM1 channels by high concentrations of 2-APB appears to involve a direct block at the channel level and an additional uncoupling of STIM1 and CRACM1, since the compound reversed the store-dependent multimerization of STIM1. Finally, we demonstrate that single-point mutations of critical amino acids in the selectivity filter of the CRACM1 pore (E106D and E190A) enable 2-APB to gate CRACM1 in a STIM1-independent manner, suggesting that 2-APB facilitates CRAC channels by altering the pore architecture.

2-Aminoethoxydiphenyl borate (2-APB) was originally introduced as an inhibitor of inositol 1,4,5-trisphosphate receptors (Maruyama *et al.* 1997), but has subsequently been found to affect a variety of ion channels. For example, the compound can inhibit TRPC3 (Trebak *et al.* 2002) and TRPV6 (Voets *et al.* 2001), and it can activate TRPV1, TRPV2, TRPV3 (Hu *et al.* 2004), as well as TRPM6 (Li *et al.* 2006). The compound has also been reported to inhibit SERCA pumps at high concentrations (Missiaen *et al.* 2001; Bilmen *et al.* 2002; Peppiatt *et al.* 2003). Probably the

most reliable and best-studied effect of 2-APB, however, is its ability to affect store-operated Ca^{2+} entry (SOCE) by modulating CRAC channel activity. Its effects are bimodal, with low concentrations facilitating and high concentrations inhibiting the calcium release-activated calcium current I_{CRAC} in various cell types of the immune system such as Jurkat T cells, DT40 B cells and RBL cells (Kukkonen *et al.* 2001; Prakriya & Lewis, 2001; Ma, 2002).

The molecular components of I_{CRAC} have been identified, with STIM1 and STIM2 (stromal interaction molecules) acting as Ca^{2+} sensors in the endoplasmic reticulum (ER) and CRACM1, CRACM2 and CRACM3 (also known as Orai1–3) representing the plasma membrane-resident CRAC channels (Roos *et al.* 2005;

C. Peinelt and A. Lis contributed equally to this work.

This paper has online supplemental material.

Zhang *et al.* 2005; Feske *et al.* 2006; Soboloff *et al.* 2006*b*; Vig *et al.* 2006*b*; Yeromin *et al.* 2006; Parvez *et al.* 2008). Recent work has shown that both STIM proteins and all three CRAC channel proteins can interact with each other (Peinelt *et al.* 2006; Lis *et al.* 2007) and that 2-APB has differential effects on the three CRAC channel subtypes. CRAC currents activated through STIM1 and carried by CRACM1 and CRACM2 are initially facilitated and then blocked by 50 μM 2-APB, with CRACM1 being more sensitive to inhibition. In contrast, CRACM3 is greatly facilitated by 50 μM 2-APB without being inhibited. However, CRACM1 channels, when coupled to STIM2 are greatly potentiated by 2-APB with extremely rapid kinetics of activation (Parvez *et al.* 2008).

We have now examined the complex pharmacological profile of 2-APB by a careful and comprehensive analysis of its action on defined molecular components of I_{CRAC} in HEK293 cells expressing STIM1 and CRACM1, 2 and 3. We demonstrate that 2-APB, in addition to inhibiting store-operated and STIM1-activated CRAC channels, can also activate CRACM1 and CRACM3, but not CRACM2, in a store- and STIM1-independent way. This is accompanied by a drastic change of channel selectivity, producing a leftward shift in reversal potential with enormous outward currents at positive membrane voltages (up to nearly 1 nA pF^{-1} for CRACM3). 2-APB also affects STIM1 in that it reverses puncta formation following store depletion, suggesting that some of its inhibitory effects on CRACM1 are caused by uncoupling STIM1 from CRAC channels.

Methods

Subcloning and overexpression

Full-length human CRACM1, CRACM2 and CRACM3 were subcloned as described earlier (Lis *et al.* 2007). For electrophysiological analysis, CRACM proteins were over-expressed in HEK293 cells stably expressing STIM1 (Soboloff *et al.* 2006*a*) using Lipofectamine 2000 (Invitrogen) and the green fluorescent protein (GFP)-expressing cells were selected by fluorescence. Experiments were performed 24–72 h post transfection.

Electrophysiology

Patch-clamp experiments were performed in the tight-seal whole-cell configuration at 21–25°C. High-resolution current recordings were acquired using an EPC-9 patch-clamp amplifier (HEKA). Voltage ramps of 50 ms duration spanning a range of −150 to +150 mV were delivered from a holding potential of 0 mV at a rate of 0.5 Hz over a period of 100–300 s. All voltages were corrected for a liquid junction potential of 10 mV. Currents were filtered at 2.9 kHz and digitized at 100 μs intervals. Capacitive currents were determined

and corrected before each voltage ramp. Extracting the current amplitude at −80 mV, +80 mV and +130 mV from individual ramp current records assessed the low-resolution temporal development of currents. Where applicable, statistical errors of averaged data are given as means ± S.E.M. with *n* determinations. Standard external solutions were as follows (in mM): 120 NaCl, 2 MgCl$_2$, 10 CaCl$_2$, 10 TEA-Cl, 10 Hepes, 10 glucose, pH 7.2 with NaOH, 300 mosmol l^{-1}. In one experiment of Fig. 4, a Na$^+$-free solution, where NaCl was replaced equimolarly by tetraethylammonium chloride (TEA-Cl), was applied. For Ca^{2+}-free external solutions CaCl$_2$ was omitted, but Mg^{2+} was retained. In some experiments, 2-aminoethoxydiphenyl borate (2-APB) was added to the standard external solution at a final concentration as indicated. Standard internal solutions were as follows (in mM): 120 caesium glutamate, 20 Cs·BAPTA, 3 MgCl$_2$, 10 Hepes, 0.02 *myo*-inositol 1,4,5-trisphosphate (IP$_3$), pH 7.2 with CsOH, 300 mosmol l^{-1}. In one experiment of Fig. 4*B*, 120 caesium glutamate was replaced by 120 potassium glutamate and K·BAPTA was used instead of Cs·BAPTA. [Ca^{2+}]$_i$ was buffered to defined levels using 20 mM Cs·BAPTA and appropriate concentrations of CaCl$_2$ as calculated with WebMaxC (http://www.stanford.edu/~cpatton/webmaxcS.htm). All chemicals were purchased from Sigma-Aldrich Co.

Fluorescence measurements

For Ca^{2+} measurements, fura-2 AM (the acetoxymethyl ester form of fura-2; Molecular Probes, Eugene, OR, USA)-loaded cells (1 μM/60 min/37°C/in media) were kept in extracellular saline as described for electrophysiological experiments. Ca^{2+} entry was induced by application of 50 μM 2-APB in external Ringer solution via a wide-tipped application pipette directly onto the cell. In some experiments 1 mM carbachol and 50 μM 2-APB in Ca^{2+}-free external Ringer was applied. The cytosolic Ca^{2+} concentration of individual cells was monitored at a rate of 5 Hz with a dual excitation fluorometric system using a Zeiss Axiovert 200 fluorescence microscope equipped with a ×40 LD AchroPlan objective. The monochromatic light source (monochromator B, TILL-Photonics) was tuned to excite fura-2 fluorescence at 360 and 390 nm for 20 ms each. Emission was detected at 450–550 nm with a photomultiplier, whose analog signals were sampled and processed by X-Chart software (HEKA). Fluorescence ratios (F_{360}/F_{390}) were translated into free intracellular Ca^{2+} concentration based on calibration parameters derived from patch-clamp experiments with calibrated Ca^{2+} concentrations.

Confocal analysis

HEK293 cells were transfected for 4 h with 1 μg cDNA of STIM1 (C-terminal tagged with yellow fluorescent protein

(YFP)) using 5 μl Lipofectamine 2000. After replating and an additional 24 h, cells were incubated with 2 μM thapsigargin and 10 min later with 50 μM 2-APB. At each experimental step, cells were fixed for 20 min with 4% paraformaldehyde (in PBS), washed with PBS and mounted onto coverslips with Crystal/Mount (Biomeda, Foster City, CA, USA). Fluorescence images of the HEK293 cells transiently expressing YFP-tagged STIM1 were taken at a Zeiss 5 Pascal confocal laser scanning microscope, using a ×63 Zeiss Plan-Apochromat oil immersion objective. For excitation of YFP, the 488 nm line of an argon laser was used and emission was detected with a 505 nm long-pass filter. Pictures were taken with a ×2 additional zoom at a resolution of 1024 × 1024 pixels (pixel size 0.09 μm) and a pinhole of 150 μm (optical slice 1.1 μm). To improve signal-to-noise ratio, 2–4 pictures were averaged.

Results

Differential effects of 2-APB on CRACM1, CRACM2 and CRACM3

To assess the pharmacological effects of 2-APB on CRAC channels, we first determined the changes in intracellular

Ca^{2+} concentration ([Ca^{2+}]$_i$) of fura-2-loaded, intact and resting HEK293 cells in the absence or presence of STIM and CRACM proteins when exposed to 2-APB without a store-depleting stimulus. In wild-type HEK293 or cells overexpressing STIM1 alone, 2-APB application did not lead to changes in [Ca^{2+}]$_i$ (Fig. 1D). However, cells overexpressing CRACM1 or CRACM3 alone did respond with significant increases in [Ca^{2+}]$_i$ to ~250 nM and ~1 μM, respectively, whereas CRACM2-overexpressing cells were essentially unaffected by 2-APB (Fig. 1A–C). The Ca^{2+} mobilization by 2-APB was dose-dependent, with half-maximal effective concentrations (EC$_{50}$) of 2-APB-induced changes in [Ca^{2+}]$_i$ via CRACM1 and CRACM3 of 20 ± 1 μM for CRACM1 and 14 ± 4 μM for CRACM3 (Fig. 1F).

These results are somewhat surprising, since 50 μM 2-APB has been shown to completely inhibit store-operated CRACM1 currents (Peinelt *et al.* 2006; Lis *et al.* 2007) and the facilitatory effect of 2-APB on CRACM3 has so far only been described for STIM1-activated CRACM3 currents. It is also apparent that this facilitatory effect of 2-APB occurs in the absence of any significant store depletion, since CRACM2-expressing and wild-type cells failed to generate Ca^{2+} signals, and the effect is also independent of overexpressed STIM1. Since these
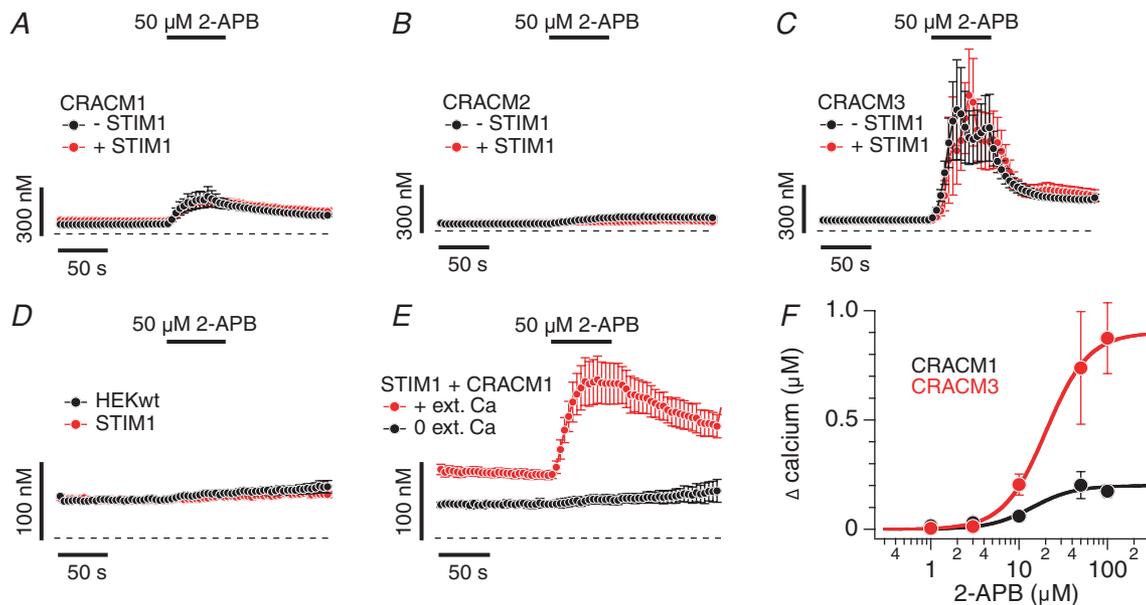
**Figure 1. Changes in intracellular calcium concentration induced by 2-APB**
A, average changes in [Ca^{2+}]$_i$ induced by 50 μM 2-APB in HEK293 wild-type (wt) cells (black: $n = 13$) and stably STIM1-expressing HEK293 cells (red: $n = 7$), both transiently overexpressing CRACM1. *B*, same as *A* for CRACM2 (black: $n = 13$; red: $n = 13$). *C*, same as *A* for CRACM3 (black: $n = 16$; red: $n = 14$). *D*, average changes in [Ca^{2+}]$_i$ induced by 50 μM 2-APB in HEK293 wt cells (black: $n = 10$) and stably STIM1-expressing HEK293 cells (red: $n = 4$). *E*, average changes in [Ca^{2+}]$_i$ induced by 50 μM 2-APB in stably STIM1-expressing HEK293 cells transiently overexpressing CRACM1 (red: $n = 7$, same as in *A*) and in Ca^{2+}-free Ringer solution (blue: $n = 4$). *F*, concentration–response curves of average changes in [Ca^{2+}]$_i$ induced by 2-APB in HEK293 cells transiently overexpressing CRACM1 (black, 2-APB: 1 μM ($n = 12$), 3 μM ($n = 10$), 10 μM ($n = 9$), 50 μM ($n = 13$), 100 μM ($n = 11$)) and CRACM3 (red, 2-APB: 1 μM ($n = 4$), 3 μM ($n = 6$), 10 μM ($n = 5$), 50 μM ($n = 16$), 100 μM ($n = 6$)). CRACM1 EC$_{50}$ = 20 ± 1 μM, Hill coefficient = 1.8; CRACM3 EC$_{50}$ = 14 ± 4 μM, Hill coefficient = 1.8.

cells express endogenous STIM molecules and 2-APB has been reported to inhibit SERCA pumps in some cell types (Missiaen *et al.* 2001; Bilmen *et al.* 2002; Peppiatt *et al.* 2003), we considered the possibility that the 2-APB-induced changes in $[Ca^{2+}]_i$ seen with CRACM1 might involve store depletion. We therefore probed store contents in CRACM1-expressing cells by first stimulating them with 2-APB in Ca^{2+}-containing media, which resulted in the small increase in $[Ca^{2+}]_i$ due to Ca^{2+} entry, and then stimulated cells with carbachol (CCh) in Ca^{2+}-free solution to activate endogenous muscarinic receptors that cause IP_3-induced release of Ca^{2+} from intracellular stores. CCh produced a very robust Ca^{2+} release signal (see Fig. S1 in online Supplemental material), demonstrating that under our experimental conditions in HEK293 cells, 2-APB does not significantly affect store contents. These results therefore indicate that 2-APB can directly and strongly activate CRACM3, while CRACM2 is resistant to this pharmacological effect. The weak activation of CRACM1 could be due to a direct, but weaker effect on the channel similar to CRACM3, or alternatively involve CRACM1 channels that are pre-coupled to endo-

genous STIM2 molecules in a store-independent manner (Parvez *et al.* 2008).

The additional overexpression of STIM1 with any of the CRAC channel subtypes, which is known to greatly amplify store-operated CRAC currents (Peinelt *et al.* 2006; Lis *et al.* 2007), did not significantly increase the response of either CRACM subtype to 2-APB application in intact cells with replete stores (Fig. 1*A–C*). To confirm that the increases in $[Ca^{2+}]_i$ were in fact due to Ca^{2+} entry via CRACM channels in the plasma membrane, we applied 50 μM 2-APB in Ca^{2+}-free extracellular solution. This indeed suppressed the 2-APB-mediated changes in $[Ca^{2+}]_i$ (Fig. 1*E*), establishing that they were caused by store-independent Ca^{2+} entry through CRAC channels.

Next we investigated membrane currents in whole-cell patch-clamp experiments, where cytosolic Ca^{2+} levels were clamped to ~150 nM using appropriate mixtures of BAPTA and $CaCl_2$. Under these conditions, Ca^{2+} stores remain filled, similar to the situation in intact resting cells. The average current densities at −80 mV and +80 mV and current–voltage relationships of CRACM1, CRACM2 and CRACM3 are shown in Fig. 2. Consistent
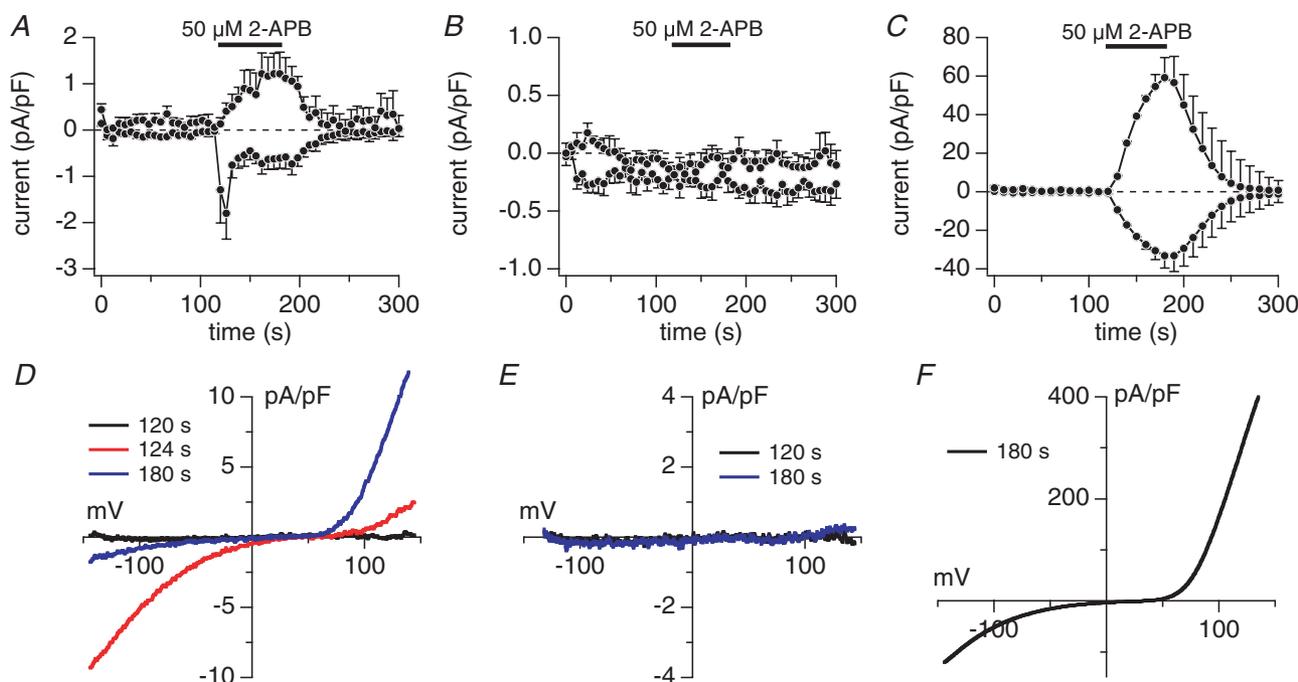
Figure 2. Comparison of CRAC currents induced by 2-APB in HEK293 wt cells transiently overexpressing CRACM1, CRACM2 or CRACM3
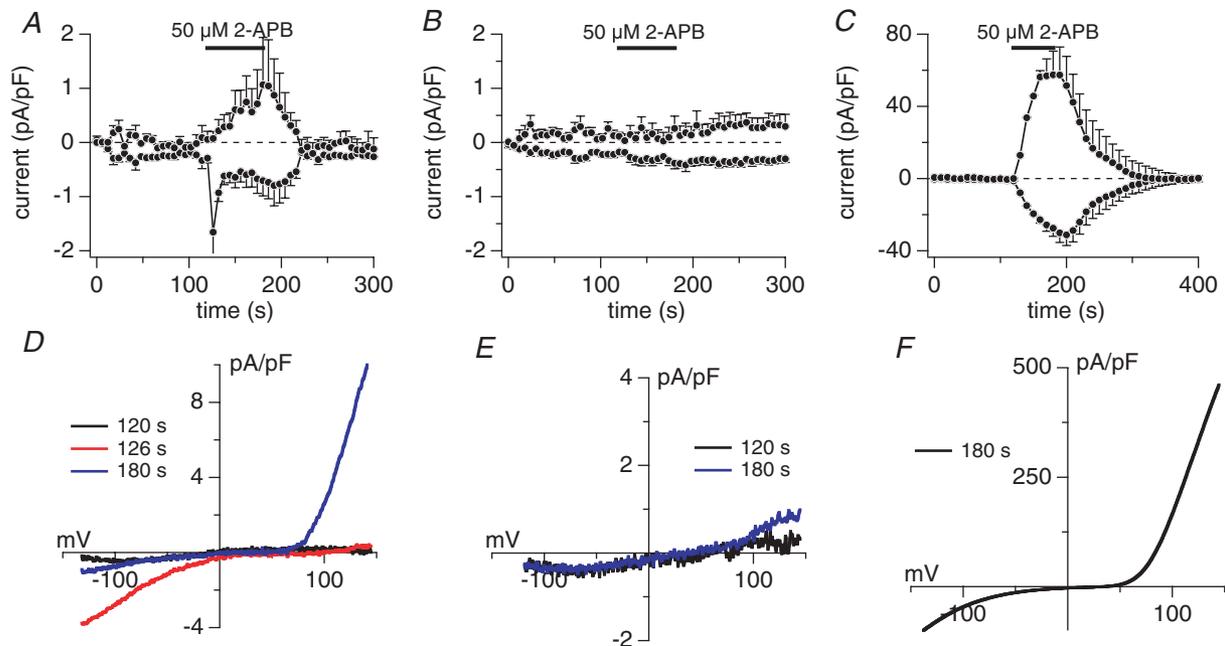*A*, average normalized currents at −80 mV and +80 mV in stable HEK293 wt cells transiently overexpressing CRACM1 (*n* = 5) without IP_3. $[Ca^{2+}]_i$ was clamped to 150 nM with 20 mM BAPTA and 8 mM $CaCl_2$. Currents of individual cells were normalized to the cell size, averaged and plotted *versus* time. The bar indicates application of external solution containing 50 μM 2-APB. *B*, same as in *A* for CRACM2 (*n* = 6). *C*, same as in *A* for CRACM3 (*n* = 5). *D*, average *I–V* relationships of CRACM1 currents extracted from representative cells at 120 s (black), 124 s (red) and 180 s (blue), when 50 μM 2-APB was applied at 120–180 s (*n* = 5). Data represent leak-subtracted current densities (pA pF^{-1}) evoked by 50 ms voltage ramps from −150 to +150 mV. *E*, same as *D* for CRACM2 at *t* = 120 s and 180 s (*n* = 6). *F*, same as *D* for CRACM3 at *t* = 180 s (*n* = 5).

with the observations in intact cells, the application of 50 μM 2-APB to CRACM1-overexpressing cells produced a small current spike of ~2 pA pF^{-1} (Fig. 2A and D) that was followed by a smaller sustained current and CRACM3-overexpressing cells generated a very large and sustained current that returned to baseline levels upon removal of 2-APB (Fig. 2C and F). As in the intact cells, CRACM2-overexpressing cells failed to respond to 2-APB (Fig. 2B and E). Since the cells were perfused with solutions containing ~150 nM free Ca^{2+}, the 2-APB-induced currents in CRACM1 and CRACM3 must have activated store-independently, in much the same way as the cells investigated with fura-2 shown in Fig. 1. Interestingly, the 2-APB-induced currents through CRACM1 and CRACM3 feature different rectification to those activated by store depletion via IP$_3$. While the current–voltage relationships of 2-APB-mediated CRAC currents reveal a reversal potential of ~30 mV for both CRACM1 and CRACM3, a significant outward component develops at positive voltages, which is ~10 pA pF^{-1} for CRACM1 and ~400 pA pF^{-1} for CRACM3 (assessed at 130 mV). This will be further addressed below.

Since the above experiments were performed under conditions of replete stores, we addressed the question of whether IP$_3$-induced store depletion had any effect on the pharmacological profile of 2-APB-induced currents through CRACM1, 2 and 3. As illustrated in Fig. 3, when intracellular Ca^{2+} stores were depleted by perfusing cells with 20 μM IP$_3$, we obtained essentially identical results to those shown in Fig. 2 for replete stores. Hence, without overexpressed STIM1, the 2-APB-induced currents via CRACM1 and CRACM3 were store-independent, whereas CRACM2 did not detectably respond to 2-APB application.

2-APB activates CRACM3 and alters its selectivity

The above results demonstrate that CRACM1 and CRACM3 can be activated in a store-independent manner by 2-APB (Figs 2 and 3). The facilitatory effects as well as the changes in the current–voltage relationship are qualitatively similar for the two subtypes, but CRACM3 features a significantly larger facilitation and an immensely

Figure 3. Comparison of CRAC currents induced by 2-APB in HEK293 wt cells transiently overexpressing CRACM1, CRACM2 or CRACM3
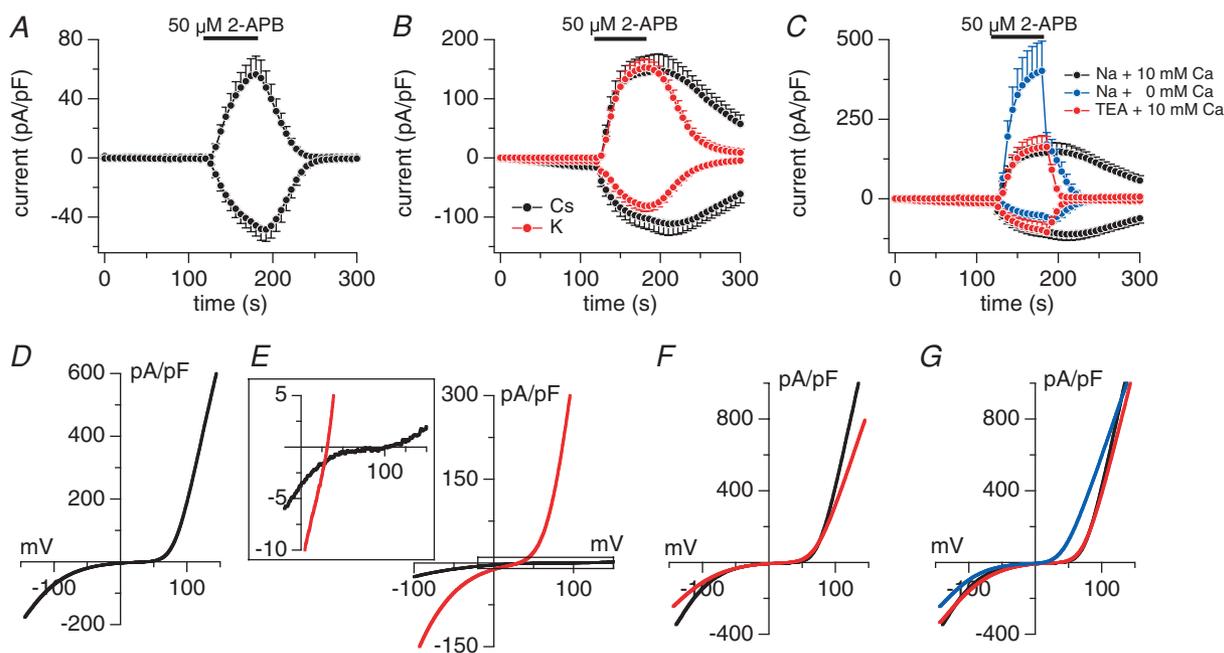
A, average normalized CRAC currents at −80 mV and +80 mV induced by IP$_3$ (20 μM) in stable HEK293 wt cells transiently overexpressing CRACM1 ($n = 7$). Currents of individual cells were normalized to the cell size, averaged and plotted *versus* time. [Ca^{2+}]$_i$ was clamped to near zero with 20 mM BAPTA. The bar indicates application of external solution containing 50 μM 2-APB. B, same as in A for CRACM2 ($n = 12$). C, same as in A for CRACM3 ($n = 12$). D, average I–V relationships of CRACM1 currents extracted from representative cells at 120 s (black), 126 s (red) and 180 s (blue), when 50 μM 2-APB was applied at 120–180 s ($n = 4$). Data represent leak-subtracted current densities (pA pF^{-1}) evoked by 50 ms voltage ramps from −150 to +150 mV. E, same as D for CRACM2 at $t = 120$ s and 180 s ($n = 4$). F, same as D for CRACM3 at $t = 180$ s ($n = 11$).

large outward component. We therefore examined the pharmacological effects of 2-APB on CRACM3 in more detail.

HEK293 cells overexpressing CRACM3 were patch-clamped with pipette solutions in which the Ca^{2+} concentration was clamped to ~150 nM in order to prevent store depletion and additionally contained 50 μM 2-APB to assess whether 2-APB can activate the channel when administered intracellularly. Under these conditions, no store-operated or 2-APB-induced current was elicited; however, when 50 μM 2-APB was applied from the outside, it readily activated CRAC currents carried by CRACM3 (Fig. 4A). This would suggest that the facilitatory effect of 2-APB either is mediated through an extracellular site on the protein or that 2-APB acts within the membrane, but cannot access its site of action from the intracellular space.

The current–voltage relationship of the 2-APB-evoked current (Fig. 4D) exhibited significant rectification at negative and positive membrane voltages with a reversal

potential of +30 mV, indicating that the selectivity of the channel had changed. Normally, CRAC currents are highly Ca^{2+}-selective and poorly permeable to K^+ or Cs^+, resulting in positive reversal potentials (Hoth & Penner, 1992, 1993). The outward currents observed when exposing cells to 2-APB, however, revealed a significant increase in monovalent Cs^+ permeation and a large shift in reversal potential. We assessed this more quantitatively in STIM1-expressing cells that were additionally transfected with CRACM3 and measured CRAC currents evoked by IP_3 with intracellular solutions containing either Cs^+ or K^+ as main monovalent cation species. Under these conditions, we observed CRAC currents due to IP_3-induced store depletion prior to 2-APB application and their average reversal potential was +100 mV ($n = 4$). 2-APB application produced large outward currents in both Cs^+- and K^+-based solutions and shifted the reversal potential to +31 mV for Cs^+ ($n = 4$) and 29 mV for K^+. The average 2-APB-mediated current in these cells was approximately twice as large compared to

Figure 4. 2-APB-induced current carried by CRACM3
A, average normalized CRAC currents at −80 mV and +80 mV in HEK293 wt cells transiently overexpressing CRACM3. Internal solution was buffered to 150 nM [Ca^{2+}]$_i$ and contained 50 μM 2-APB. The bar indicates application of 50 μM 2-APB ($n = 5$). B, average normalized CRAC currents at −80 mV and +80 mV in STIM1 cells transiently overexpressing CRACM3. Internal solution was buffered to zero [Ca^{2+}]$_i$ and contained 20 μM IP_3. The bar indicates application of 50 μM 2-APB. Internal solution contained caesium glutamate (black, $n = 9$) or potassium glutamate (red, $n = 5$). C, average normalized CRAC currents at −80 mV and +80 mV in STIM1 cells transiently overexpressing CRACM3. Internal solution was buffered to zero [Ca^{2+}]$_i$ and contained 20 μM IP_3. The bar indicates application of 50 μM 2-APB in Ca^{2+}-containing Na$^+$-Ringer solution (black, $n = 9$, same data as in B), Ca^{2+}-free Na$^+$-Ringer solution (blue, $n = 5$), or Ca^{2+}-containing TEA-Ringer solution (red, $n = 5$). D, example I–V curve for data shown in A at the end of 2-APB application (180 s). E, average example I–V curves for Cs^+ data set shown in B ($n = 4$). The black trace indicates CRAC currents measured before application of 2-APB (120 s), the red trace was obtained at the end of application (180 s). The magnified and boxed inset exemplifies the shift in reversal potential caused by 2-APB (from ~100 mV to 31 mV, respectively).

CRACM3 currents without STIM1 overexpression. This would indicate that both store-operated and STIM 1-activated channels as well as store-independent and STIM1-uncoupled populations of CRACM3 channels exhibit the 2-APB-mediated facilitation. However, it is possible that true facilitation of CRACM3 currents might in fact be larger than apparent from the twofold increase if 2-APB also concurrently inhibits the coupling between STIM1 and CRACM3, as it does in the case of CRACM1 and CRACM2 (see below).

Although 2-APB shifted the reversal potential of CRAC currents, it remained at positive potentials, suggesting that the channels retained some Ca^{2+} permeability, consistent with the Ca^{2+} entry observed in fura-2 measurements in intact cells (see Fig. 1). We investigated monovalent *versus* divalent cation permeation in ion substitution experiments, where either Ca^{2+} was removed from the extracellular solution or Na^+ was replaced by TEA. As illustrated in Fig. 4*C*, application of 2-APB in Ca^{2+}-free extracellular solution reduced the average inward current by 53% compared to Ca^{2+}-containing solutions, but nearly tripled the outward current. This was accompanied by a shift in reversal potential from +94 mV to +10 mV. This would suggest that Ca^{2+} is responsible for a significant portion of the inward current and that it also impedes the outward movement of monovalent cations. At the same time, it is apparent that in the presence of 2-APB, CRAC channels are significantly more permeable to Na^+ ions, since normally, Ca^{2+}-free solutions completely suppress any inward currents through CRAC channels (Hoth & Penner, 1992).

Conversely, removing Na^+ from the extracellular solution by replacing it with TEA^+ had no significant effect on inward or outward currents induced by 50 μM 2-APB. When considering the ionic concentrations and valencies of these ions, CRAC channels retain preferential permeation of Ca^{2+} over Na^+. Goldman–Hodgkin–Katz analysis of the reversal potentials in Fig. 4*G* yielded permeability ratios of $P_{Na}/P_{Cs} = 1.5$ under Ca^{2+}-free conditions (blue *I–V*, $E_{rev} = +10$ mV) and $P_{Ca}/P_{Cs} = 50$ (red *I–V*, +30 mV), which indicates a value of $P_{Ca}/P_{Na} = 33$. This formal method of assessing permeability ratios may not be entirely accurate, as it is based on the assumption that transport of one ion species takes place independently of other ions, which we know is not the case, since Ca^{2+} impedes monovalent cation transport. Nevertheless, it is clear that 2-APB causes a dramatic reduction in CRAC channel selectivity, as normally, CRAC channels feature P_{Ca}/P_{Na} in excess of 100-fold (Hoth & Penner, 1992; Zweifach & Lewis, 1993).

Figure S2 in the online Supplemental material summarizes the current densities of the 2-APB-mediated in- and outward currents observed with CRACM3 under various conditions. Changes in external or internal solution composition do slightly change conductivities of the 2-APB-induced CRACM3 current, but preserve the unique pharmacological addition of a large outward current at positive membrane voltages. The graph also includes data from cells in which CRACM3 was coexpressed with STIM1 (see below). This generated larger currents, but also preserved the general behaviour in terms of selectivity and *I–V* relationships.

2-APB inhibits STIM1-mediated gating of CRACM1 and CRACM2 but not CRACM3

The above results are mainly concerned with the facilitatory effects of 2-APB on CRAC currents in the absence of STIM1 overexpression; however, 2-APB normally has a bimodal action on native CRAC currents, which are activated by STIM1 in a store-dependent manner. Here, 2-APB concentrations below 5 μM typically facilitate and higher concentrations block the currents (Kukkonen *et al.* 2001; Prakriya & Lewis, 2001; Ma, 2002). We therefore assessed the pharmacological profile of 2-APB on all three CRAC channel subtypes in the additional presence of STIM1.

As illustrated in Fig. 5, we performed a full dose–response analysis of 2-APB on IP_3-induced currents via CRACM1, 2 or 3 when expressed in HEK293 cells that stably expressed STIM1. Cells were exposed to various concentrations of 2-APB after CRAC currents had fully developed following IP_3-mediated store depletion. All three CRAC channel subtypes exhibited facilitation of inward currents at low micromolar concentrations (Fig. 5*A–C*). At higher concentrations, the facilitation was seen as a transient increase in current that was followed by inhibition in CRACM1 and CRACM2, whereas CRACM3 remained facilitated and showed no obvious signs of inhibition, although some inhibition might have been masked by facilitation.

Figure 5*G* (CRACM1) and Fig. 5*H* (CRACM2) show the *I–V* relationships of IP_3-induced I_{CRAC} (black), facilitated (red) and blocked (blue) current for application of 50 μM 2-APB. We analysed the current responses by plotting the facilitated peak current relative to the normalized current before 2-APB application and the steady-state inhibited current relative to the facilitated peak to estimate the dose–response behaviour of facilitation and inhibition. The resulting dose–response curves of CRACM1 (Fig. 5*D*), CRACM2 (Fig. 5*E*) and CRACM3 (Fig. 5*F*) show that the facilitation of all three subtypes is achieved with half-maximal effective concentrations (EC_{50}) of 4 μM, 6 μM and 15 μM for CRACM1, CRACM2 and CRACM3, respectively. In parallel, CRACM1 and CRACM2, but not CRACM3, were also inhibited with similar half-maximal inhibitory concentrations (IC_{50}) of 8 μM and 6 μM, respectively. Remarkably, though, the overall potency of 2-APB in inhibiting CRACM1 and CRACM2 was quite

different, as CRACM1 currents were blocked by ~95% at concentrations above 10 μM, whereas CRACM2 currents were only suppressed by ~40% even at the highest concentrations.

These differences in inhibitory potency may also affect the overall efficacy and potency of 2-APB in mediating the facilitatory effects and could explain the seemingly smaller maximal magnitude of CRACM1 facilitation (~60%) compared to CRACM2 (~120%). Thus, the slightly higher

efficacy of CRACM1 and CRACM2 facilitation compared to CRACM3 may be overestimated, since the maximal facilitation is reached at lower concentrations, where the inhibitory effect is limiting a further increase in current amplitude. This effect is particularly strong for CRACM1, which is more potently inhibited than CRACM2 and we therefore surmise that its true facilitation may in fact be on a par with, if not larger than, that seen with CRACM3.
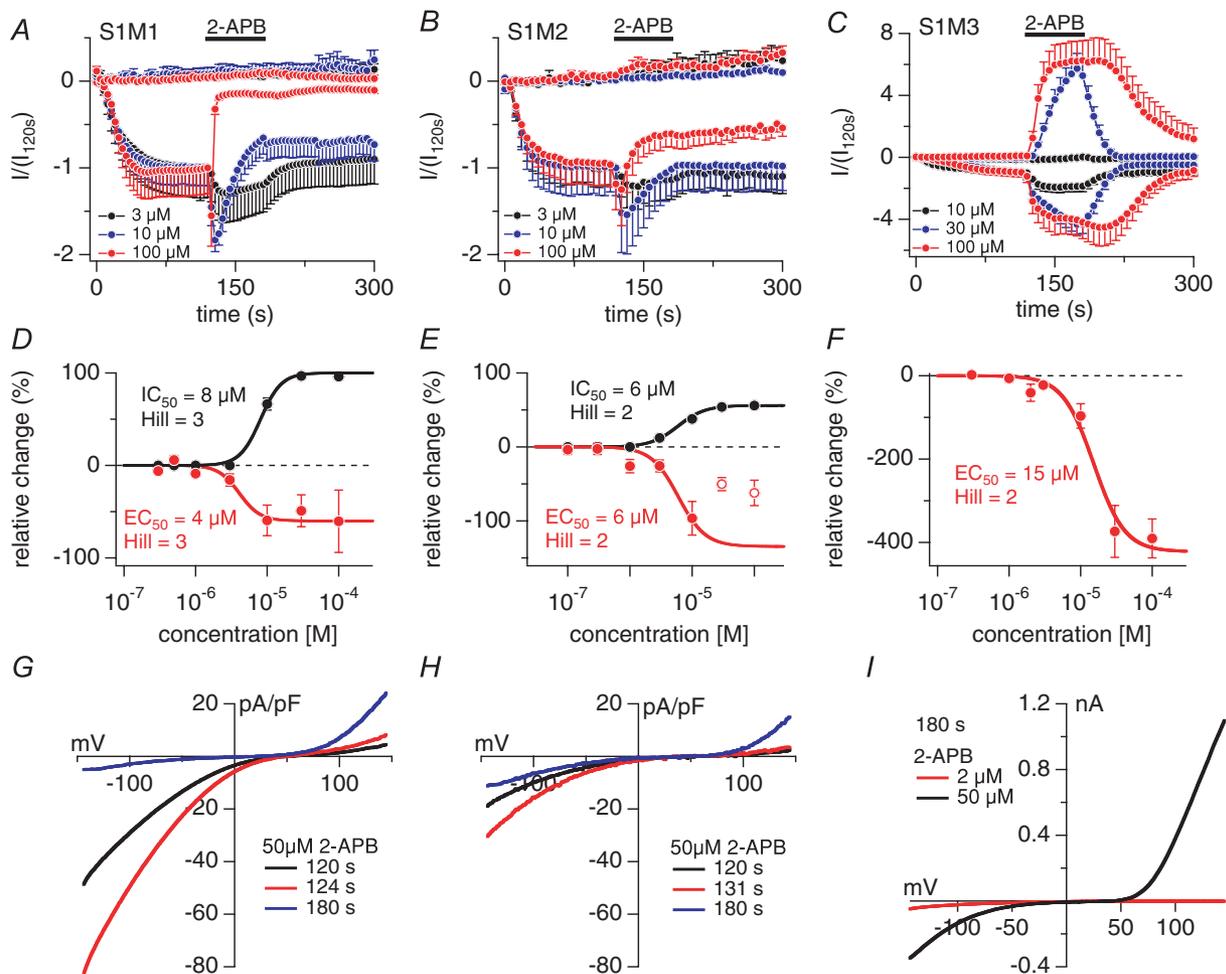
Figure 5. 2-APB dose response
A, average normalized CRAC currents at −80 mV and +80 mV induced by 20 μM IP$_3$ in stable STIM1-expressing HEK293 cells transiently overexpressing CRACM1. Currents of individual cells were normalized to the current before solution change at 120 s (I/I_{120s}). [Ca^{2+}]$_i$ was clamped to near zero with 20 mM BAPTA. The bar indicates application of external solution containing 3 μM ($n = 5$), 10 μM ($n = 5$), or 100 μM ($n = 5$) 2-APB. *B*, same as *A* for CRACM2. The bar indicates application of external solution containing 3 μM ($n = 9$), 10 μM ($n = 8$), or 100 μM ($n = 6$) 2-APB. *C*, same as *A* for CRACM3. The bar indicates application of external solution containing 10 μM ($n = 8$), 30 μM ($n = 8$) or 100 μM ($n = 8$) 2-APB. *D*, dose response of 2-APB on CRACM1. The IC$_{50}$ for the block is 8 μM and the EC$_{50}$ for the amplification 4 μM. *E*, dose response of 2-APB on CRACM2. The IC$_{50}$ for the block is 6 μM and the EC$_{50}$ for the amplification is 6 μM. *F*, dose response of 2-APB on CRACM3. The EC$_{50}$ for the amplification is 15 μM. *G*, average *I–V* relationships of CRACM1 currents extracted from representative cells at 120 s, 124 s and 180 s ($n = 11$), when 50 μM 2-APB was applied at 120–180 s. Data represent leak-subtracted current densities (pA pF^{-1}) evoked by 50 ms voltage ramps from −150 to +150 mV. *H*, same as *G* for CRACM2 at 120 s, 132 s and 180 s ($n = 4$). *I*, same as *G* for CRACM3 at 180 s, when 2 μM ($n = 5$) or 50 μM ($n = 5$) 2-APB was applied.

Since the above experiments revealed both facilitation and inhibition of CRACM1 by 2-APB when STIM1 was coexpressed, we wondered whether both effects occurred at the channel level or, alternatively, facilitation occurred at the channel and inhibition was imparted by inhibition of the coupling between STIM1 and the channel. One of the hallmarks of STIM1-dependent activation of CRAC channels is that upon store depletion, STIM1 multimerizes and aggregates into puncta underneath the plasma membrane (Liou *et al.* 2005; Roos *et al.* 2005) and reversal of puncta formation is a prerequisite for termination of SOCE (Smyth *et al.* 2008). We assessed the effects of 2-APB on puncta formation through confocal microscopy in HEK293-expressing YFP-tagged STIM1. Consistent with numerous previous studies, STIM1 is relatively evenly distributed across the ER at rest (Fig. 6*A*) and forms punctate structures after cells are exposed to thapsigargin (Fig. 6*B*). Subsequent application of 50 μM 2-APB essentially reverses the punctate staining and STIM1 distribution returns to a state where it is indistinguishable from resting cells. This clearly suggests, that 2-APB can affect STIM1 and at least part of the inhibitory effects seen on CRACM1 currents may be attributable to reversal of STIM1 puncta formation.

2-APB activates CRACM1 pore mutants

The above results demonstrate that 2-APB alters the selectivity of CRAC channels and it is conceivable that the mechanism by which 2-APB gates CRACM3 channels is linked to a widening of the selectivity filter, so that ions can permeate without the requirement of store depletion or STIM1 interaction. The degree of pore widening could determine the efficacy of 2-APB in gating the

CRAC channel subtypes, with CRACM3 being the most susceptible, CRACM1 being just barely activatable, and CRACM2's pore being insufficiently widened by 2-APB to allow the passage of ions without STIM1. Previous work has identified glutamate residues E106 in transmembrane domain TM1 and E190 in TM3 as critical determinants of the selectivity of the CRACM1 pore (Prakriya *et al.* 2006; Vig *et al.* 2006a; Yeromin *et al.* 2006). We considered the possibility that pore mutants with altered pore architecture might respond differently to 2-APB and selected two CRACM1 mutants (E106D and E190A) to test for 2-APB susceptibility. The E106D mutant of CRACM1 converts the normally inwardly rectifying channel into outwardly rectifying and shifts its reversal potential to +16 mV (Prakriya *et al.* 2006; Vig *et al.* 2006a; Yeromin *et al.* 2006), but has no constitutive channel activity and requires additional STIM1 overexpression and store depletion to produce large CRAC currents, suggesting that a simple alteration of pore selectivity does not result in store-independent gating.

We confirmed that HEK293 expressing the E106D mutant of CRACM1 alone had no constitutive CRAC currents and subsequent challenge with 50 μM 2-APB produced a complex response that typically produced a rapid increase in inward current, followed by complete block, and a slow reactivation after 2-APB application was suspended (Fig. 7*A*). A simple interpretation of this observation would be that CRACM1 channels initially activate as the 2-APB concentration builds up around the channel, but are then blocked as more 2-APB molecules accumulate. After stopping 2-APB application, 2-APB molecules diffuse away and the local concentration decreases so that the CRAC channels can reactivate. The magnitude of the reactivated currents surpasses that of currents normally seen in cells that express
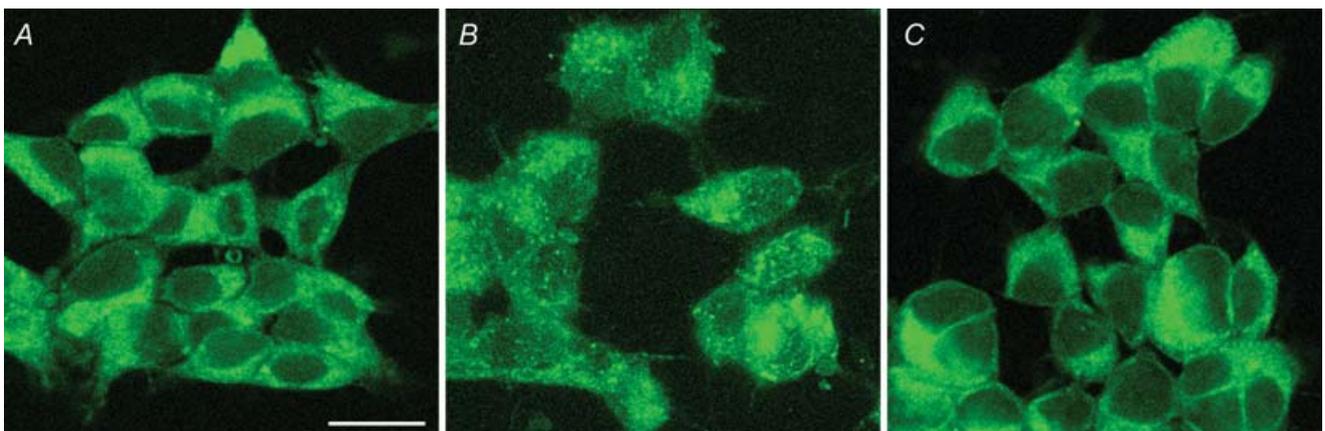

Figure 6. Confocal fluorescence images of YFP-tagged STIM1 transiently expressed in HEK293 cells
A, resting cells prior to stimulation. *B*, 10 min after incubation with 2 μM thapsigargin STIM1 aggregates into puncta. *C*, 10 min after incubation of cells with 50 μM 2-APB thapsigargin-induced puncta formation is reversed. Scale bar in *A* represents 20 μm.

CRACM1 channels alone in the absence of additional STIM1 overexpression, indicating that they result from store- and STIM1-independent gating of CRACM1. The current–voltage relationship of the reactivated current is essentially linear with a reversal potential of 0 mV (Fig. 7*B*), suggesting that 2-APB further shifts the reversal potential of the E106D mutant from +16 mV to the left.

We next assessed the E190 residue of CRACM1, which is also important for CRAC channel selectivity. When this glutamate residue is mutated to glutamine (E190Q), it shifts the reversal potential of the current to +50 mV and the *I–V* curve exhibits both inward and outward rectification (Vig *et al.* 2006*a*). The E190Q mutant was marginally effective in restoring SOCE in T cells with defective Ca^{2+} influx derived from SCID (severe combined immunodeficiency) patients, whereas E190A and E190D mutants fully restored Ca^{2+} influx (Prakriya *et al.* 2006). We investigated the E190A mutant, which has not yet been characterized electrophysiologically. Figure 7*C* illustrates

that when this mutant is coexpressed with STIM1, it responds similarly to wild-type CRACM1 when IP_3 is perfused into cells. It activated rapidly following store depletion and its *I–V* relationship was similar to that of wild-type channels in that it exhibited strong inward rectification (Fig. 7*D*), although its reversal potential was shifted to +55 mV, similar to the E190Q mutant. Thus, this mutant appears to have an intermediate phenotype in that it also changes the selectivity of CRACM1, but outward transport of Cs^+ appears to be significantly less than seen with the E190Q mutant. When exposing cells to 50 μM 2-APB after CRAC currents had fully activated, the compound evoked a large facilitation followed by rapid inhibition (Fig. 7*C*), qualitatively similar to wild-type CRACM1, but with a more pronounced facilitation. The facilitated current was characterized by a larger outward current and a leftward shift in reversal potential to +33 mV (Fig. 7*D*), again demonstrating that 2-APB lowers the selectivity of CRAC channels.
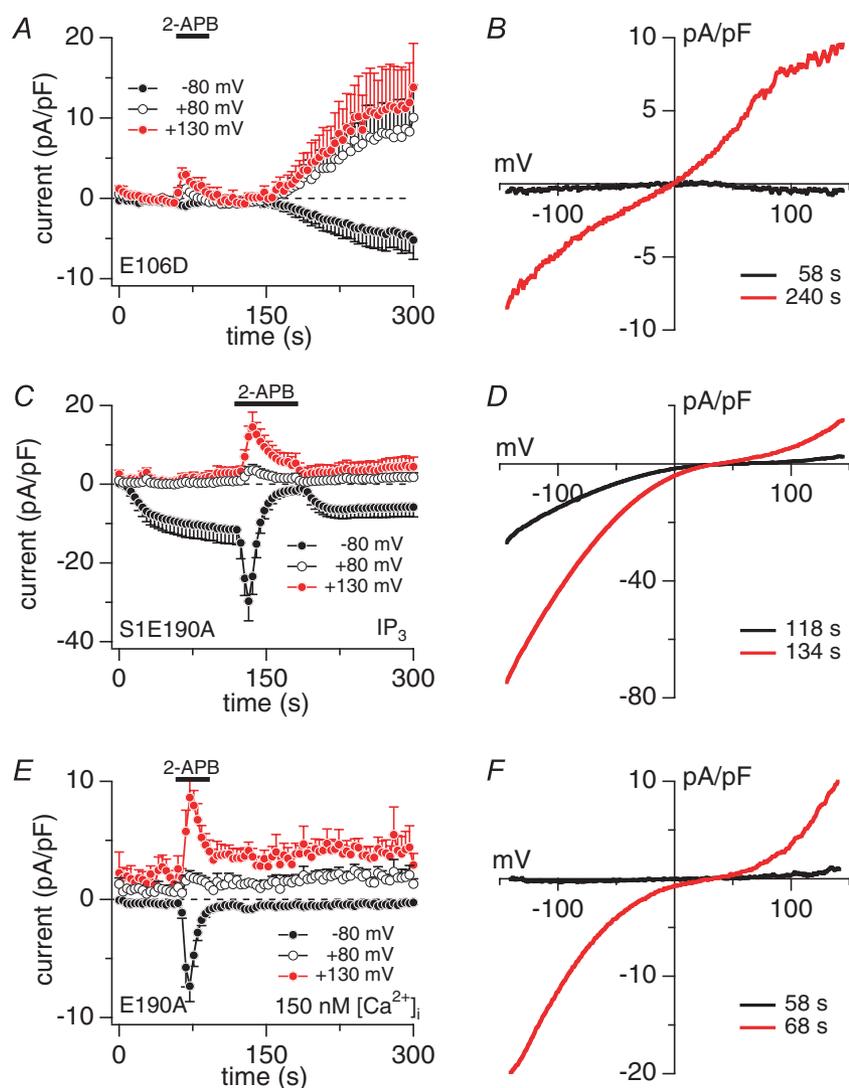
Figure 7. 2-APB-induced current via CRACM1 pore mutants

A, average normalized CRAC currents at −80 mV (black), +80 mV (open symbols) and +130 mV (red) in HEK293 wt cells transiently overexpressing CRACM1-E106D. Internal solution was buffered to 150 n$_M$ Ca^{2+}. The bar indicates application of external solution containing 50 μM 2-APB (*n* = 5). *B*, example *I–V* curves for the data set shown in *A* prior to 2-APB application and during CRAC reactivation. *C*, average normalized CRAC currents at −80 mV (black), +80 mV (open symbols) and +130 mV (red) in HEK293 stably expressing STIM1 and transiently overexpressing CRACM1-E190A. Internal solution contained 20 μM IP_3. The bar indicates application of external solution containing 50 μM 2-APB (*n* = 9). *D*, example *I–V* curves for the data set shown in *C* prior to 2-APB application and at the peak of CRAC current facilitation. *E*, average normalized CRAC currents at −80 mV (black), +80 mV (open symbols) and +130 mV (red) in HEK293 wt cells transiently overexpressing CRACM1-E190A. Internal solution was buffered to 150 n$_M$ Ca^{2+}. The bar indicates application of external solution containing 50 μM 2-APB (*n* = 8). *F*, example *I–V* curves for the data set shown in *A* prior to 2-APB application and at the peak of CRAC current facilitation.

We next analysed the effect of 2-APB on the E190A mutant when expressed alone, without STIM1, in wild-type HEK293 cells. In these experiments, we also omitted IP$_3$ from the pipette solution and buffered $[Ca^{2+}]_i$ to ~150 nM to avoid store depletion. Indeed, this completely suppressed the development of any currents following establishment of the whole-cell configuration (Fig. 7E). Application of 50 μM 2-APB, however, produced a large, transient increase in both inward and outward current, whose I–V relationship (Fig. 7F) was similar to that observed in Fig. 7D where 2-APB facilitated store-operated E190A channels coexpressed with STIM1. Taken together, these data suggest that wild-type CRACM1 channels are largely resistant to store- and STIM1-independent gating by 2-APB, but modifications of residues E106 and E190, while not sufficient to gate the channel in a constitutive manner, enable 2-APB to further modify the pore architecture of CRACM1 so that the channels open in a store- and STIM1-independent manner. The results also suggest that this gating mode is favoured at low 2-APB concentrations that build up at the start of 2-APB application and as the concentration in the membrane increases may transition into a state that no longer allows ion transport. Thus, 2-APB can both facilitate and inhibit CRAC channel function directly without requiring STIM1 overexpression. The inhibitory effect may act in combination with the reversal of STIM1 puncta formation.

Discussion

In summary, this study provides a thorough analysis of the pharmacological profile of 2-APB, revealing several new and surprising insights into the mechanisms that result in the complex regulation of CRAC channel subtypes. The most significant observation was that 2-APB can activate CRACM3 channels in a store-independent manner and without the requirement of STIM proteins, resulting in enormous CRAC currents. By contrast, CRACM2 by itself was completely unresponsive to 2-APB; however, when coexpressed with STIM1 and activated via store depletion, this CRAC channel subtype was facilitated at low 2-APB concentrations and inhibited at higher concentrations. CRACM1 by itself, while also largely unresponsive to 2-APB stimulation, did exhibit a small but consistent facilitation that was followed by inhibition when using high concentrations of 2-APB. In addition, the 2-APB-induced CRACM currents exhibit an altered selectivity that manifests itself in a leftward shift in reversal potential and the emergence of large outward currents that are carried by the normally impermeant monovalent cations Cs^+ and K^+. We further demonstrate that pore mutants of CRACM1 become susceptible to STIM1-independent gating, suggesting that the pore architecture is crucially involved in 2-APB-mediated

facilitation. The inhibitory effect of 2-APB appears to be mediated both at the channel level, as observed for CRACM1 currents in cells without STIM1 overexpression, and at the STIM1 level, as evidenced by the reversal of store-dependent puncta formation in thapsigargin-treated cells.

The dual effect of 2-APB on gating and a concomitant change in selectivity of CRAC channels is surprising and may be caused by two separate mechanisms or by a single mechanism where gating and selectivity are coupled processes. There is some evidence that C-type inactivation of K^+ channels and Ca^{2+}-dependent inactivation of voltage-dependent Ca^{2+} channels may be mediated by changes in the channels' selectivity filter that obstruct ion permeation (Starkus *et al.* 1997; Kiss & Korn, 1998; Babich *et al.* 2005, 2007). A similar mechanism has been proposed for Ca^{2+}-dependent inactivation of CRAC channels based on the observation that mutations in the putative selectivity filter of CRACM1 also affect fast Ca^{2+}-dependent inactivation (Yamashita, 2007), although none of the CRAC channel mutations described so far can obviate the requirement for store depletion to open the channel. Interestingly, the changes in selectivity produced by 2-APB on CRACM1 and CRACM3 described in the present study are very similar to the changes in selectivity seen with the E190Q mutation of CRACM1 (Prakriya *et al.* 2006; Vig *et al.* 2006*a*; Yeromin *et al.* 2006). It is conceivable that the mechanism by which 2-APB gates CRACM3 channels and the pore mutants of CRACM1 is linked to its insertion into the plasma membrane, binding to the transmembrane regions of CRAC channels, and causing a widening of the selectivity filter, so that ions can permeate without the requirement of store depletion or STIM1 interaction. The degree of pore widening could determine the efficacy of 2-APB in gating the CRAC channel subtypes, with CRACM3 being the most susceptible, CRACM1 being somewhat activatable, and CRACM2's pore being insufficiently widened by 2-APB to allow the passage of ions without STIM1. It is important to note, however, that a change in selectivity of the CRAC channel pore, such as, e.g. mediated by the E106D or E190Q mutants, does not seem to be sufficient to enable STIM-independent gating.

Thus, all three CRAC channel subtypes can in principle be facilitated by 2-APB; however, while CRACM3 is facilitated independently of STIM1 and store depletion, wild-type CRACM1 and CRACM2 require both factors for facilitation. Interestingly, the latter two subtypes are also subject to 2-APB-mediated inhibition when exposed to high concentrations of the compound, indicating that the presence of STIM1 may at least in part be responsible for the inhibitory effect. Our observation that 2-APB can reverse the thapsigargin-induced formation of puncta is consistent with this notion. Since the

kinetics of this effect is slower and occurs at higher concentrations of 2-APB, it may contribute to a biphasic change in CRAC channel activity with initial facilitation followed by subsequent inhibition. The question then arises whether 2-APB also affects the interaction of STIM1 with CRACM3. Although the net effect of 2-APB on CRACM3 is facilitatory, it is possible that some degree of inhibition also occurs, but is not obvious due to the massive facilitation.

If the assumption that the facilitation is mediated at the CRAC channel and the inhibition is a consequence of the disruption of STIM and CRAC channel interaction, we need to explain why CRACM1 is both facilitated and inhibited even when STIM1 is not overexpressed (see Fig. 2*A*). This could be due to endogenous STIM2 molecules that are pre-coupled to CRACM1. We have previously demonstrated that CRACM1 and STIM2 can be massively facilitated in the absence of store depletion (Parvez *et al.* 2008) and we have attributed this effect to the presence of constitutively coupled STIM2–CRACM1 complexes that are inhibited by calmodulin. It is therefore conceivable that the overexpression of CRACM1 channels, without additional STIM1 overexpression and in the absence of store depletion, nevertheless results in their constitutive coupling with the limited number of endogenous STIM2 molecules and so accounts for the small facilitatory and inhibitory response observed. In this scenario, the inability of CRACM2, which can also couple to STIM2 (Parvez *et al.* 2008), to produce a similar response may be due to a less efficient constitutive coupling to CRACM2 with STIM2. In fact, we have previously reported that, while store-dependent activation of all three CRAC channel subtypes by STIM2 is similar, the proportion of constitutively coupled STIM2–CRACM2 complexes is much smaller than that of STIM2–CRACM1 (Parvez *et al.* 2008).

An alternative explanation for the 2-APB-mediated effects on wild-type CRACM1 could be that the facilitation and subsequent inhibition are STIM-independent and both are mediated at the channel level. This scenario is plausible in light of the experiments involving CRACM1 pore mutants. Here, we found that single-point mutations of glutamate residues E106 and E190 within the selectivity filter at the outer mouth of the pore of CRACM1 confer 2-APB-mediated gating in the absence of STIM1 overexpression or store depletion and this gating is followed by a rapid inhibition. We propose that E106D and E190A mutants of CRACM1 alter the pore architecture of CRACM1 sufficiently so that further 2-APB-induced conformational changes enable STIM1-independent channel opening. As more 2-APB molecules interact with CRAC channels, the channel may transition into a conformational state that prevents ion transport. Of course, it is also possible that both STIM-dependent and STIM-independent mechanisms act in synergy to inhibit CRAC channel function.

Our results highlight the complexities of 2-APB action on CRAC channels. The differential facilitatory effects on CRAC channel subtypes that are accompanied, or possibly caused, by a change in channel selectivity, and the concomitant inhibitory effect on STIM1-mediated gating may explain some of the variability of 2-APB responses reported in the literature. Future work involving site-directed mutagenesis of CRAC and STIM proteins should reveal further insights into the molecular sites involved in mediating these effects.

References

Babich O, Isaev D & Shirokov R (2005). Role of extracellular Ca^{2+} in gating of $Ca_V 1.2$ channels. *J Physiol* **565**, 709–715.

Babich O, Matveev V, Harris AL & Shirokov R (2007). Ca^{2+}-dependent inactivation of $Ca_V 1.2$ channels prevents Gd^{3+} block: does Ca^{2+} block the pore of inactivated channels? *J Gen Physiol* **129**, 477–483.

Bakowski D, Glitsch MD & Parekh AB (2001). An examination of the secretion-like coupling model for the activation of the Ca^{2+} release-activated Ca^{2+} current I (CRAC) in RBL-1 cells. *J Physiol* **532**, 55–71.

Bakowski D, Parekh AB (2007). Voltage-dependent Ba^{2+} permeation through store-operated CRAC channels: implications for channel selectivity. *Cell Calcium* **42**, 333–339.

Bilmen JG, Wootton LL, Godfrey RE, Smart OS & Michelangeli F (2002). Inhibition of SERCA Ca^{2+} pumps by 2-aminoethoxydiphenyl borate (2-APB). 2-APB reduces both Ca^{2+} binding and phosphoryl transfer from ATP, by interfering with the pathway leading to the Ca^{2+}-binding sites. *Eur J Biochem* **269**, 3678–3687.

Feske S, Gwack Y, Prakriya M, Srikanth S, Puppel SH, Tanasa B, Hogan PG, Lewis RS, Daly M & Rao A (2006). A mutation in Orai1 causes immune deficiency by abrogating CRAC channel function. *Nature* **441**, 179–185.

Hoth M & Penner R (1992). Depletion of intracellular calcium stores activates a calcium current in mast cells. *Nature* **355**, 353–356.

Hoth M & Penner R (1993). Calcium release-activated calcium current in rat mast cells. *J Physiol* **465**, 359–386.

Hu HZ, Gu Q, Wang C, Colton CK, Tang J, Kinoshita-Kawada M, Lee LY, Wood JD & Zhu MX (2004). 2-Aminoethoxydiphenyl borate is a common activator of TRPV1, TRPV2, and TRPV3. *J Biol Chem* **279**, 35741–35748.

Kiss L & Korn SJ (1998). Modulation of C-type inactivation by K^+ at the potassium channel selectivity filter. *Biophys J* **74**, 1840–1849.

Kukkonen JP, Lund PE & Akerman KE (2001). 2-Aminoethoxydiphenyl borate reveals heterogeneity in receptor-activated Ca^{2+} discharge and store-operated Ca^{2+} influx. *Cell Calcium* **30**, 117–129.

Li M, Jiang J & Yue L (2006). Functional characterization of homo- and heteromeric channel kinases TRPM6 and TRPM7. *J Gen Physiol* **127**, 525–537.

Liou J, Kim ML, Heo WD, Jones JT, Myers JW, Ferrell JE Jr & Meyer T (2005). STIM is a Ca^{2+} sensor essential for Ca^{2+}-store-depletion-triggered Ca^{2+} influx. *Curr Biol* **15**, 1235–1241.

Lis A, Peinelt C, Beck A, Parvez S, Monteilh-Zoller M, Fleig A & Penner R (2007). CRACM1, CRACM2, and CRACM3 are store-operated Ca^{2+} channels with distinct functional properties. *Curr Biol* **17**, 794–800.

Maruyama T, Kanaji T, Nakade S, Kanno T & Mikoshiba K (1997). 2APB, 2-aminoethoxydiphenyl borate, a membrane-penetrable modulator of Ins(1,4,5)P_3-induced Ca^{2+} release. *J Biochem* **122**, 498–505.

Missiaen L, Callewaert G, De Smedt H & Parys JB (2001). 2-Aminoethoxydiphenyl borate affects the inositol 1,4,5-trisphosphate receptor, the intracellular Ca^{2+} pump and the non-specific Ca^{2+} leak from the non-mitochondrial Ca^{2+} stores in permeabilized A7r5 cells. *Cell Calcium* **29**, 111–116.

Parvez S, Beck A, Peinelt C, Soboloff J, Lis A, Monteilh-Zoller M, Gill DL, Fleig A & Penner R (2008). STIM2 protein mediates distinct store-dependent and store-independent modes of CRAC channel activation. *FASEB J* **22**, 752–761.

Peinelt C, Vig M, Koomoa DL, Beck A, Nadler MJ, Koblan-Huberson M, Lis A, Fleig A, Penner R & Kinet JP (2006). Amplification of CRAC current by STIM1 and CRACM1 (Orai1). *Nat Cell Biol* **8**, 771–773.

Peppiatt CM, Collins TJ, Mackenzie L, Conway SJ, Holmes AB, Bootman MD, Berridge MJ, Seo JT & Roderick HL (2003). 2-Aminoethoxydiphenyl borate (2-APB) antagonises inositol 1,4,5-trisphosphate-induced calcium release, inhibits calcium pumps and has a use-dependent and slowly reversible action on store-operated calcium entry channels. *Cell Calcium* **34**, 97–108.

Prakriya M, Feske S, Gwack Y, Srikanth S, Rao A & Hogan PG (2006). Orai1 is an essential pore subunit of the CRAC channel. *Nature* **443**, 230–233.

Prakriya M & Lewis RS (2001). Potentiation and inhibition of Ca^{2+} release-activated Ca^{2+} channels by 2-aminoethyldiphenyl borate (2-APB) occurs independently of IP$_3$ receptors. *J Physiol* **536**, 3–19.

Roos J, DiGregorio PJ, Yeromin AV, Ohlsen K, Lioudyno M, Zhang S, Safrina O, Kozak JA, Wagner SL, Cahalan MD, Velicelebi G & Stauderman KA (2005). STIM1, an essential and conserved component of store-operated Ca^{2+} channel function. *J Cell Biol* **169**, 435–445.

Smyth JT, Dehaven WI, Bird GS & Putney JW Jr (2008). Ca^{2+}-store-dependent and -independent reversal of Stim1 localization and function. *J Cell Sci* **121**, 762–772.

Soboloff J, Spassova MA, Hewavitharana T, He LP, Xu W, Johnstone LS, Dziadek MA & Gill DL (2006a). STIM2 is an inhibitor of STIM1-mediated store-operated Ca^{2+} entry. *Curr Biol* **16**, 1465–1470.

Soboloff J, Spassova MA, Tang XD, Hewavitharana T, Xu W & Gill DL (2006b). Orai1 and STIM reconstitute store-operated calcium channel function. *J Biol Chem* **281**, 20661–20665.

Starkus JG, Kuschel L, Rayner MD & Heinemann SH (1997). Ion conduction through C-type inactivated *Shaker* channels. *J Gen Physiol* **110**, 539–550.

Trebak M, Bird GS, McKay RR & Putney JW Jr (2002). Comparison of human TRPC3 channels in receptor-activated and store-operated modes. Differential sensitivity to channel blockers suggests fundamental differences in channel composition. *J Biol Chem* **277**, 21617–21623.

Vig M, Beck A, Billingsley JM, Lis A, Parvez S, Peinelt C, Koomoa DL, Soboloff J, Gill DL, Fleig A, Kinet JP & Penner R (2006a). CRACM1 multimers form the ion-selective pore of the CRAC channel. *Curr Biol* **16**, 2073–2079.

Vig M, Peinelt C, Beck A, Koomoa DL, Rabah D, Koblan-Huberson M, Kraft S, Turner H, Fleig A, Penner R & Kinet JP (2006b). CRACM1 is a plasma membrane protein essential for store-operated Ca^{2+} entry. *Science* **312**, 1220–1223.

Voets T, Prenen J, Fleig A, Vennekens R, Watanabe H, Hoenderop JG, Bindels RJ, Droogmans G, Penner R & Nilius B (2001). CaT1 and the calcium release-activated calcium channel manifest distinct pore properties. *J Biol Chem* **276**, 47767–47770.

Yamashita M, Navarro-Borelly L, McNally BA & Prakriya M (2007). Orai1 mutations alter ion permeation and Ca^{2+} dependent fast inactivation of CRAC channels: evidence for coupling of permeation and gating. *JGP* **130**, 525–540.

Yeromin AV, Zhang SL, Jiang W, Yu Y, Safrina O & Cahalan MD (2006). Molecular identification of the CRAC channel by altered ion selectivity in a mutant of Orai. *Nature* **443**, 226–229.

Zhang SL, Yu Y, Roos J, Kozak JA, Deerinck TJ, Ellisman MH, Stauderman KA & Cahalan MD (2005). STIM1 is a Ca^{2+} sensor that activates CRAC channels and migrates from the Ca^{2+} store to the plasma membrane. *Nature* **437**, 902–905.

Zweifach A & Lewis RS (1993). Mitogen-regulated Ca^{2+} current of T lymphocytes is activated by depletion of intracellular Ca^{2+} stores. *Proc Natl Acad Sci U S A* **90**, 6295–6299.

Author's present address

C. Peinelt: Department of Biophysics, Medical Faculty, Saarland University, Homburg, Germany.

Supplemental material

Online supplemental material for this paper can be accessed at: http://jp.physoc.org/cgi/content/full/jphysiol.2008.151365/DC1 and

http://www.blackwell-synergy.com/doi/suppl/10.1113/jphysiol.2008.151365